

Behavior of bubbles in cylindrical fluidized beds at an elevated temperature

メタデータ	言語: eng 出版者: 公開日: 2011-06-24 キーワード (Ja): キーワード (En): 作成者: HATATE, Yasuo, OMAGARI, Koji, IKARI, Atsushi, KONDO, Kazuo, King, Desmond F. メールアドレス: 所属:
URL	http://hdl.handle.net/10232/11430

BEHAVIOR OF BUBBLES IN CYLINDRICAL FLUIDIZED BEDS AT AN ELEVATED TEMPERATURE

Yasuo HATATE, Kohji OHMAGARI, Atsushi IKARI
Kazuo KONDO* and Desmond F. King**

(Received May 30, 1987)

The effect of temperature on bubble size in gassolid fluidized beds was investigated using two kinds of cylindrical beds of 147 and 256 mm in diameter each, and spherical glass beads of 272 μm in average size as fluidized particles under the following operating conditions;

excess gas velocity=1–8cm/s,
static bed height=10–42cm,
and temperature=300 and 600 K.

The following results were obtained.

1. The bubble diameter at 600 K is larger than that at 300 K. However, this difference becomes small when the excess gas velocity is increased above minimal values.
2. The effect of column diameter on the bubble diameter was scarcely observed. However, as expected, the larger diameter bed tends to give larger diameter bubbles in the slugging regime.

Introduction

A number of commercial fluidized beds are operated at high temperatures. To facilitate design and scale-up, it is necessary to know the behavior of fluidized beds at high temperatures. A representative study on the effect of temperature on bubble size by Yoshida et al.⁷⁾ showed a tendency for decreasing bubble size with increasing temperature. Recently, however, Stubington et al.⁵⁾ reported that in a range of temperature between 600 K and 1300 K, no measurable change in bubble size occurred although a 5 to 15% decrease in bubble size was found up to 600 K.

In a previous paper³⁾, the behavior of bubbles in a cylindrical fluidized bed with an internal diameter of 147 mm was investigated at elevated temperatures.

In the present study, to know in detail the behavior of fluidized beds at high temperatures, two cylindrical fluidized beds were used—one with an internal diameter of 147 mm and the other with an internal diameter of 256 mm. Both were equipped with a high speed video-camera system in order to investigate the behavior of swarms of bubbles.

1. Experimental

1. 1 Bed particle

Spherical glass beads shown in Table 1 were used as the bed material for the experiments. This particle belongs to "Group B" in Geldart's classification.¹⁾ Air was used as the fluidizing medium in all

*Dept. of Organic Synthesis, Kyushu Univ., Hakozaki, Higashi-ku, Fukuoka 812

**Process Design Division, Chevron Research Company, 576 Standard Ave., Richmond, California 94802, U. S. A.

Table 1. Particles

d_{p32} [μm]	U_{mf} [cm/s]		density [g/cm^3]
	300 K	600 K	
272	7.0	4.8	2.52

experiments. The volume to surface average size, d_{p32} , was determined by photography. Minimum fluidization velocity, U_{mf} , was obtained from measuring the relationship between pressure drop, ΔP , and superficial gas velocity, U_G , at each temperature.

1. 2 Cylindrical fluidized bed

A schematic diagram of the experimental apparatus for the cylindrical fluidized beds is shown in Fig. 1. One of the fluidized beds is fabricated of stainless steel with an internal diameter of 147 mm. The other is made of steel with an internal diameter of 256 mm. The smaller bed is composed of one pre-heater section with four upper cylindrical sections, the larger bed has one pre-heater section and three upper cylindrical sections. The upper cylindrical sections are removable piece by piece to change the bed height. A flat plate of pyrex glass caps the top of the upper most cylindrical section of each bed. Through this window bubbles erupting at the bed surface can be observed. Both sides of the bed are equipped with pressure taps and tubes into which thermocouples are inserted to measure bed temperature. A heater is fitted in the pre-heater section in which raschig rings are packed to ensure uniform air flow. Jacket heaters with Kaowool (ceramic fiber) are installed on the outside of the column to offset wall heat losses.

The flow rate of the air from the compressor was measured by a bank of calibrated orifice meters after oil and water had been removed by an air filter and an air-oil separator. The air from the bed was discharged through a cyclone and a vent pipe.

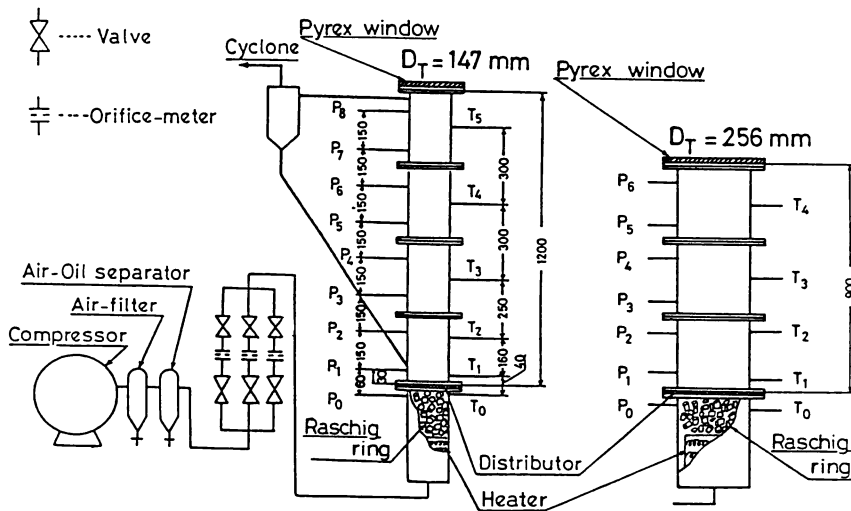


Fig. 1 Experimental apparatus

1. 3 Distributor plate

A stainless steel perforated distributor plate of thickness 5 mm was used in each bed. The distributor for the 147 mm internal diameter bed has 177 holes of 1 mm diameter arranged in square pitch. The distributor for the larger fluidized bed has 489 holes of 1 mm diameter. The hole to bed area ratio is about 0.8% for each distributor.

1. 4 Experimental procedure

After a steady state was attained for a given experimental condition, the bubbles were photographed through the pyrex glass window by a high speed video-camera system (exposure time=0.6ms, 60 frames/s) and recorded on a VTR.

1. 5 Analysis

The VTR pictures were analyzed to determine the average size of bubbles just before erupting. The longitudinal and lateral lengths of the bubbles were measured and the average value of both the lengths was taken to be the eruption diameter. The volume average calculated from these values is regarded as the average bubble size. In this study, the eruption diameter is for convenience referred to as just "bubble diameter". About one hundred bubbles were chosen for inspection for a given experimental condition.

2. Results and Discussion

The experimental conditions used are shown in Table 2.

Table 2. Experimental conditions

Static bed height	: 10, 15, 25, 30 and 42 cm
$U_G - U_{mf}$: 1, 2, 3, 4 and 8 cm/s
Temperature	: 300 and 600 K
Bed diameter	: 147 and 256 mm

The minimum fluidization velocity for the spherical glass beads was in the range of the deviation of $\pm 35\%$ from the correlation of Wen and Yu⁶⁾ expressed by Eq. (1).

$$U_{mf} = \frac{d_p^2 (\rho_p - \rho_f) g}{1650 \mu} \quad (Ar < 1.9 \times 10^4) \quad (1)$$

Figures 2 and 3 show the effect of temperature on bubble size distribution for $U_G - U_{mf} = 4.0$ cm/s, in the 147 mm diameter bed. Under these experimental conditions, about the same bubble size distributions were obtained at bed temperatures of 300 K and 600 K. In other words, a similar cluster of bubbles occurred at each temperature.

Figure 4 shows the effect of temperature on bubble diameter for various static bed heights at an excess gas velocity of 4 cm/s in the 147 mm column. The solid line in the figure shows the relationship between \bar{D}_{Er} and h_s , where \bar{D}_{Er} is 1.2 times the value of \bar{D}_E calculated by the correlation of Mori and Wen⁴⁾ given in Eq. (2).

$$D_E = D_{BM} + (D_{BO} - D_{BM}) \exp(-0.3h/D_T) \quad (2)$$

where $D_{BO} = 0.347 ((U_G - U_{mf}) A/n)^{0.4}$

$$D_{BM} = 0.652 ((U_G - U_{mf}) A)^{0.4}$$

The value of h in Eq.(2) was obtained by extrapolation from the relationship between h and Δp . It is

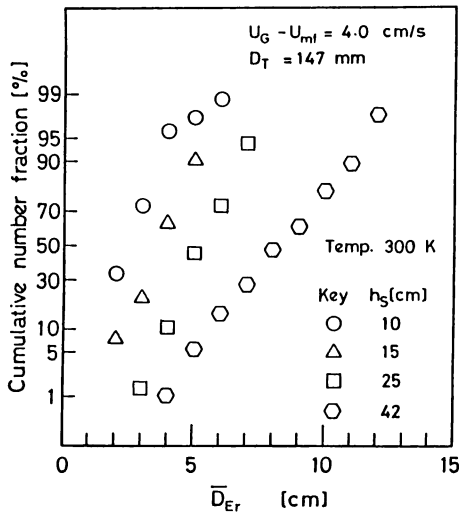


Fig. 2 Normal probability plots for \bar{D}_{Er} at various bed heights

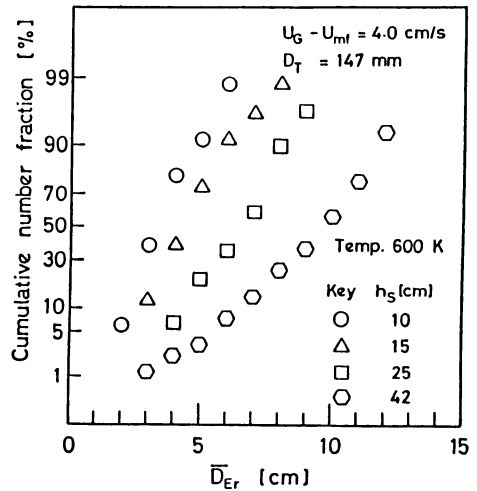


Fig. 3 Normal probability plots for \bar{D}_{Er} at various bed heights

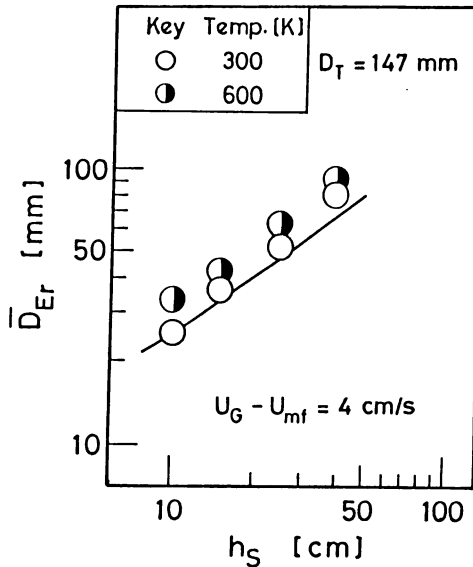


Fig. 4 Effect of temperature on \bar{D}_{Er} vs. h_s relation

apparent from the figure that the bubble diameter at 600 K is larger than that calculated by the correlation of Mori and Wen, but theory and experiment agree for the 300 K results. Moreover, at the low excess gas velocities studied, it was clearly found that bubble diameters at 600 K are larger than those at 300 K. This is believed to be caused by an increase in the frequency of bubble coalescences due to an enhancement in the motion of bubbles in the transverse direction at higher temperature, as was clarified by observation of the motion of a cluster of bubbles in a semi-cylindrical fluidized bed.²⁾ As the excess gas velocity is increased, however, the difference in bubble diameters at 600 K and 300 K is diminished. It

appears that the bubble diameter is less affected by temperature as the excess gas velocity is increased to attain slugging regimes. This is caused by the fact that coalescence of the bubbles in the transverse direction is ceased when the gas velocity is increased to some extent.

Figure 5 shows the effects of temperature and column diameter on bubble diameter for a range of excess gas velocities when the static bed height is kept constant. The solid lines in the figure show the correlation derived by Mori and Wen. Again, the bubble diameter at 600 K is larger than that at 300 K even for the 256 mm column. Furthermore, the effect of the column diameter is small at low excess gas velocity. However, as expected, the bubble diameter in the larger column is larger when the excess gas velocity is increased to attain slugging.

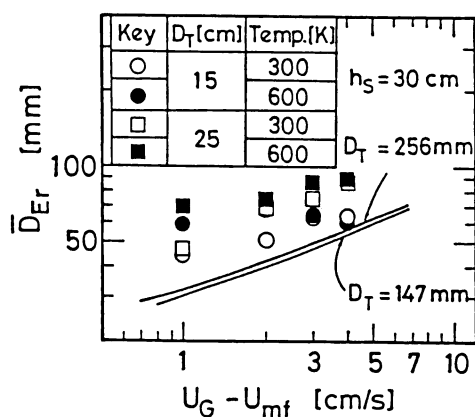


Fig. 5 Effect of temperature on \bar{D}_{Er} vs. $U_G - U_{mf}$ relation

Conclusion

Using cylindrical fluidized beds with column diameters of 147 mm and 256 mm, bubble diameters were measured at 300 K and 600 K. The following results were obtained.

- 1) Using spherical glass beads with an average diameter of $272\mu\text{m}$, the bubble diameter at 600 K is larger than that 300 K. However, this difference becomes small when the excess gas velocity is increased above minimal values.
- 2) An effect of column diameter on the bubble diameter was scarcely observed. However, as expected, the larger diameter bed tends to give larger diameter bubbles in the slugging regime.

Nomenclature

A	= cross section area of bed	[cm ²]
Ar	= Archimedes number	[-]
D_{BM}	= initial bubble diameter at distributor	[cm]
D_{BO}	= maximum bubble diameter due to total coalescence of bubbles	[cm]
D_E	= equivalent diameter of bubble	[cm]
\bar{D}_E	= volume average equivalent diameter of bubbles	[cm]
\bar{D}_{Er}	= volume average eruption diameter of bubbles	[cm]
D_T	= bed diameter	[cm]

d_{p32}	= volume to surface average diameter of particles by photographic analysis	[μm]
g	= gravitational acceleration	[cm/s^2]
h	= bed height above distributor	[cm]
h_s	= static bed height above distributor	[cm]
n	= number of orifices in distributor plate	[-]
ΔP	= pressure drop	[Pa]
U_G	= superficial gas velocity	[cm/s]
U_{mf}	= minimum fluidization velocity	[cm/s]
ρ_f	= density of fluid	[g/cm^3]
ρ_p	= density of particle	[g/cm^3]
μ	= viscosity of fluid	[$\text{Pa}\cdot\text{s}$]

Literature Cited

- 1) Geldart, D.: *Powder Technol.*, 7, 285 (1973)
- 2) Hatate, Y., M. Migita, N. Kawabata, K. Ohmagari, D. F. King and A. Ikari: *Preprint of the 19th Autumn Meeting of The Soc. of Chem. Engrs., Japan*, SL 101, Oct., 1985
- 3) Hatate, Y., K. Ohmagari, A. Ikari, K. Kondo and D. F. King: *submitted to J. Chem. Eng. Japan*
- 4) Mori, S. and C. Y. Wen: *AIChE J.*, 21, 109 (1975)
- 5) Stubington, J. F., D. Barrett and G. Lowry: *Chem. Eng. Res. Des.*, 62, 173 (1984)
- 6) Wen, C. Y. and Y. H. Yu: *AIChE J.*, 12, 610 (1966)
- 7) Yoshida, K., S. Fujii and D. Kunii: *Fluidization Technol.*, 1, 43 (1976)